

Design and Clinical Utility of a Fan Beam Collimator for SPECT Imaging of the Head

Benjamin M.W. Tsui, Grant T. Gullberg*, Eric R. Edgerton, David R. Gilland,
J. Randolph Perry, and William H. McCartney

Department of Radiology and Curriculum in Biomedical Engineering, The University of North Carolina at Chapel Hill; and General Electric Company, Medical Systems Group, Milwaukee, Wisconsin

A long bore fan beam collimator for imaging the head was designed and constructed for a SPECT system with a rotating scintillation camera. In order to avoid the patient's shoulder during rotation of the camera with a thick camera housing, the long bore design is necessary to allow the collimator to get close to the patient's head for improved spatial resolution. Operating at the minimum radius of rotation, the prototype fan beam collimator provides about the same spatial resolution as the high resolution collimator, while the geometric efficiency is equal to ~85% of that of the general purpose and ~55% higher than the high resolution collimator. Images from a phantom study demonstrate good image quality and are void of artifacts. Comparative clinical studies on temporomandibular joints (TMJ) between the LEGP and fan beam collimators also confirm the superior image quality obtained with the fan beam collimator.

J Nucl Med 27:810-819, 1986

In order to obtain the best spatial resolution in single photon emission computed tomography (SPECT) imaging, the radius of rotation should be kept at a minimum. In SPECT imaging of the head, the shoulder of the patient hinders the approach of the collimator when the camera has a thick housing. There are a few approaches to alleviate this problem, one of which is to decrease the thickness of the camera housing. This requires a change in the design of the camera and has been marketed recently by a commercial manufacturer (1). A second method is to use slant hole collimators (2). The problem with this approach is that the spatial resolution varies among different reconstruction slices due to the change of spacing between the collimator and the patient's head.

In this paper, we describe the design and investigate the clinical utility of a long bore fan beam collimator for SPECT imaging of the head. In order to avoid the

patient's shoulder during rotation, the fan beam collimator consists of long holes which protrude beyond the camera housing. To compensate for the loss of geometric efficiency due to the long hole length, the fan beam geometry proposed by Jaszczak et al. was used (3,4). The collimator holes in the transverse reconstructed image plane are tapered and converge to the same focal point. In the longitudinal direction, the collimator holes are straight and parallel for data collection of contiguous image slices.

The design is guided by a theoretic analysis of the physical characteristics of the collimator. The prototype collimator has a spatial resolution of 12 mm at 15 cm radius of rotation. The geometric efficiency is ~85% of that of the low-energy general purpose collimator (LEGP) and is about 55% higher than a parallel hole collimator design which has the same hole length and spatial resolution.

A fan beam reconstruction algorithm with attenuation correction was implemented. The parameters of the fan beam collimator and of the imaging geometry were determined and incorporated in the reconstruction algorithm. Processing time was decreased significantly by using an array processor in the image reconstruction. Phantom studies were performed to evaluate the colli-

Received Apr. 24, 1985; revision accepted Jan. 15, 1986.

For reprints contact: Dr. Tsui, Dept. of Radiology and Curriculum in Biomedical Engineering, Univ. of North Carolina at Chapel Hill, 152 MacNider Hall 202H, Chapel Hill, NC 27514.

* Present address: Department of Radiology, University of Utah, Salt Lake City, UT 84132.

mator and the reconstruction algorithm. Clinical studies of the temporomandibular joints (TMJ) showed improved diagnostic image quality obtained by using the fan beam collimator as compared to the LEGP collimator.

THEORY

Geometric Response of Converging-Hole and Fan Beam Collimators

In considering the response of a conventional parallel-hole collimator, an effective point source response function is defined as the image of a point source that would be obtained if the collimator was uniformly translated (5,6). For a camera collimator with congruent straight parallel holes and negligible septal penetration, the translation motion is equivalent to averaging the point source images formed for various positions of the collimator hole array with respect to the point source position. Thus, the effective geometric point source response function of the collimator is shift-invariant and can be determined by the geometric effects of a single hole (6).

Equivalently, for the converging hole collimator, the effective point spread function can be considered as the average of point source images formed for various rotational positions of the collimator hole array around the center hole and for various positions of the collimator hole as they move towards the center holes. Furthermore, if the hole apertures at the collimator backplane are identical, the effective point source response function can be determined by the geometric effects of a single hole.

Assuming that the point source is located at a point on the axis of the collimator and at a distance Z from the collimator face, the average photon fluence which passes through both the front and back hole apertures and reaches a point \vec{r} in the image plane is given by

$$\phi(\vec{r}) = \frac{k}{[(Z + L + B)^2 + |\vec{r}|^2]^{3/2}} \int a_b\left(-\frac{L(F - Z)}{F(Z + L + B)} \vec{r} - \vec{\rho}\right) a_b(-\vec{\rho}) d\vec{\rho}, \quad (1)$$

where $a_b(\vec{r})$ is the aperture function of the collimator hole at the backplane, L is the collimator hole length, B is the gap between the collimator backplane and the image plane in the crystal, k is a proportionality constant and the integration is taken over the entire image plane. If the dimension of the hole is small compared to the hole length L , the quantity $|\vec{r}|$ will be small compared with $(Z + L + B)$ when $\phi(\vec{r})$ is nonzero. Then, the term in front of the integral in Eq. (1) is essentially a constant.

The two-dimensional Fourier transform of $\phi(\vec{r})$ is

often easier to work with and from Eq. (1) we find

$$\Phi(\vec{\nu}) = \left| \tilde{A}_b\left(\left[-\frac{F(Z + L + B)}{L(F - Z)}\right] \vec{\nu}\right) \right|^2, \quad (2)$$

where $\tilde{A}_b(\vec{\nu}) = A_b(\vec{\nu})/A_b(0)$ is the normalized two-dimensional Fourier transform of a hole aperture at the backplane and $A_b(\vec{\nu})$ is the Fourier transform of $a_b(\vec{r})$.

The spatial resolution of the collimator in the reconstructed image planes can be represented by the line spread function measured in the plane of the converging holes. On the axis of the fan-beam geometry, the cross section of $\Phi(\vec{\nu})$ in Eq. (2) in the plane of the fan gives the Fourier transform of the corresponding line spread function. This provides a measure of the spatial resolution of the fan beam collimator. At points away from the axis of the fan beam geometry, the spatial resolution deviates from that on the axis. The deviation increases with distance from the axis of the fan beam and with decreased focal length (4).

Among different collimator holes shapes, the hexagonal hole shape gives the maximum geometric efficiency for the same average spatial resolution (7) and is chosen in our design. For ease of construction, it is best to have the planes of the converging holes parallel to a side of the hexagon of the collimator hole. The aperture function in this orientation is given by (6)

$$A(\nu) = \frac{1}{3} \left(2 \operatorname{sinc}(\sqrt{3}\beta) + \left[\operatorname{sinc}\left(\frac{\sqrt{3}\beta}{2}\right) \right]^2 \right), \quad (3)$$

where $\operatorname{sinc}(x) = \sin(x)/x$, $\beta = \pi w \nu$ and w is the width of a side of the hexagonal-shaped holes. By substituting Eq. (3) in Eq. (2), we obtain the transfer function of the collimator on the axis of the fan beam geometry and the one-dimensional Fourier transform yields the corresponding line spread function. This provides a prediction of the geometric response of the fan beam collimator as a function of the source distance and the shape, width and length of the collimator holes.

Figure 1A shows examples of the predicted spatial resolution (in terms of FWHM) as a function of source distance for three hypothetical fan beam collimator designs using Eqs. (1), (2), and (3). All three collimators have the same focal length of 58 cm, but different hole lengths and sizes to give the same spatial resolution of 9 mm at 15 cm from the collimator face.

Based on the theoretic prediction in Eqs. (1), (2), and (3), we also simulated the spatial resolution in the reconstructed image for a given source location and radius of rotation (8). In the simulation, the line source is oriented parallel to the axis of rotation. At each projection angle, the distance between the collimator and the line source is determined and the predicted line spread function is used as the projection profile. From the simulated projection data, the reconstructed image of the line source can be obtained.

The full width at half maximum (FWHM) values of

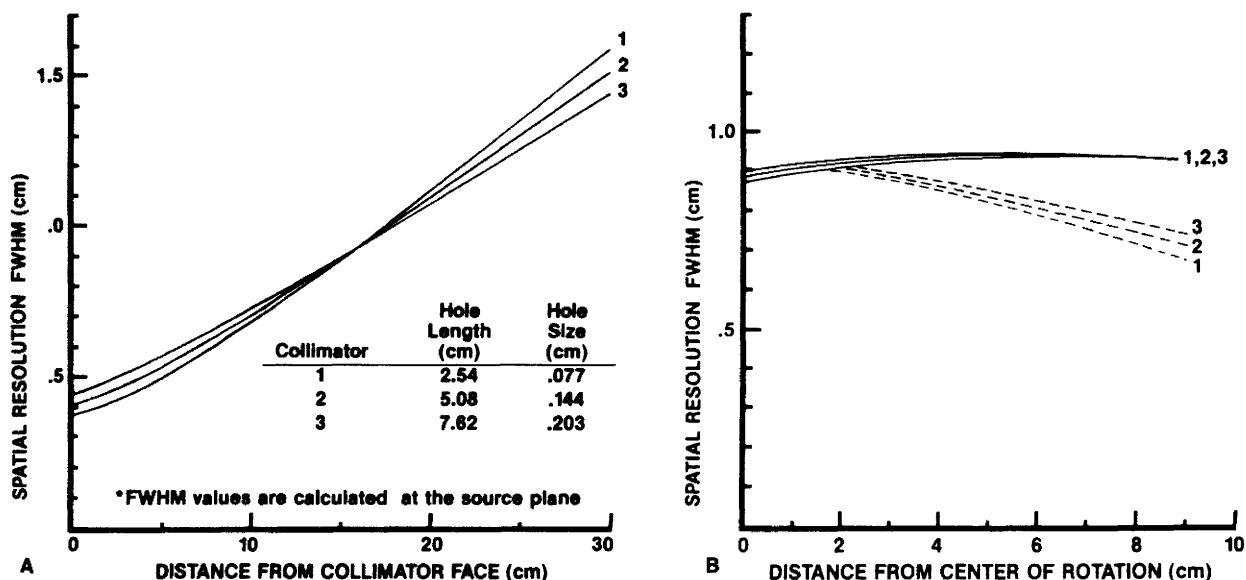


FIGURE 1

A: Predicted spatial resolution (FWHM) of line spread function of three hypothetical fan beam collimator designs as function of source distance. B: Spatial resolutions of point spread functions measured in radial (—) and tangential directions (---) in reconstructed image as function of distance from center of rotation obtained from simulations using collimators in A. Simulation assumed hexagonal hole shape and intrinsic resolution of 0.38 cm

the line source image measured tangentially and radially as a function of distance from the center of rotation are shown in Fig. 1B. For source locations away from the center of rotation, the reconstructed images of the line source are asymmetrical resulting from the variations in spatial resolution in the projection data at different angles. In general, longer collimator hole length gives rise to smaller changes in spatial resolution as function of distance from the collimator and less degree of asymmetry in the reconstructed image. Thus, collimators with longer hole length are more suitable for use in SPECT imaging (9).

Geometric Efficiency of Fan Beam Collimators

Unlike the parallel hole collimator, the geometric efficiency of a fan beam collimator is a function of the source distance Z and is approximately given by

$$G = G_0 \frac{F}{(F - Z)} \quad 0 < Z < F, \quad (4)$$

where F is the focal length of the fan. The geometric efficiency G_0 at the collimator face is given by (7)

$$G_0 = \frac{(\text{Area})_b (\text{Area})_f}{4\pi L_e^2}, \quad (5)$$

where $L_e = L - \frac{2}{\mu}$, $(\text{Area})_b$ and $(\text{Area})_f$ are the area of the back and front apertures, respectively, L and L_e are the length and effective length of the collimator holes, respectively, and μ is the attenuation coefficient of the septal material. Equation (4) shows that the geometric efficiency of the fan beam collimator increases with

shorter focal length. For a fixed focal length, the geometric efficiency increases as the source moves towards the focal point with the concurrent decrease of the image field size.

MATERIALS AND METHODS

Collimator Design for Head Tomography

Our design goal for a prototype fan beam collimator was to achieve a spatial resolution about equal to that of a high resolution collimator (HRES) at the normal operating radius of rotation while maximizing the geometric efficiency. The theoretic formulation described in the previous section was used to determine the parameters of the collimator design to achieve the above stated goals.

The dimensions of the fan beam collimator designed for the GE 400 A/T⁺ SPECT system are shown in Figs. 2A, B, and C. The collimator holes are 13 cm long with 8.5 cm extended beyond the face of the camera housing. This allows the radius of rotation to be as short as 15 cm without being obstructed by the patient's shoulders. In the transverse reconstructed image plane (Fig. 2A), that is perpendicular to the axis of rotation, the collimator holes are tapered and arranged in such a way that the hole axes are all focused to the same point. Assuming a typical patient's head with diameter equal to 20 cm is located 15 cm from the collimator face, the minimum focal length required is 58 cm. In the longitudinal direction (Fig. 2B), the walls of the collimator holes are straight and parallel such that contiguous and parallel reconstruction slices can be obtained. The area

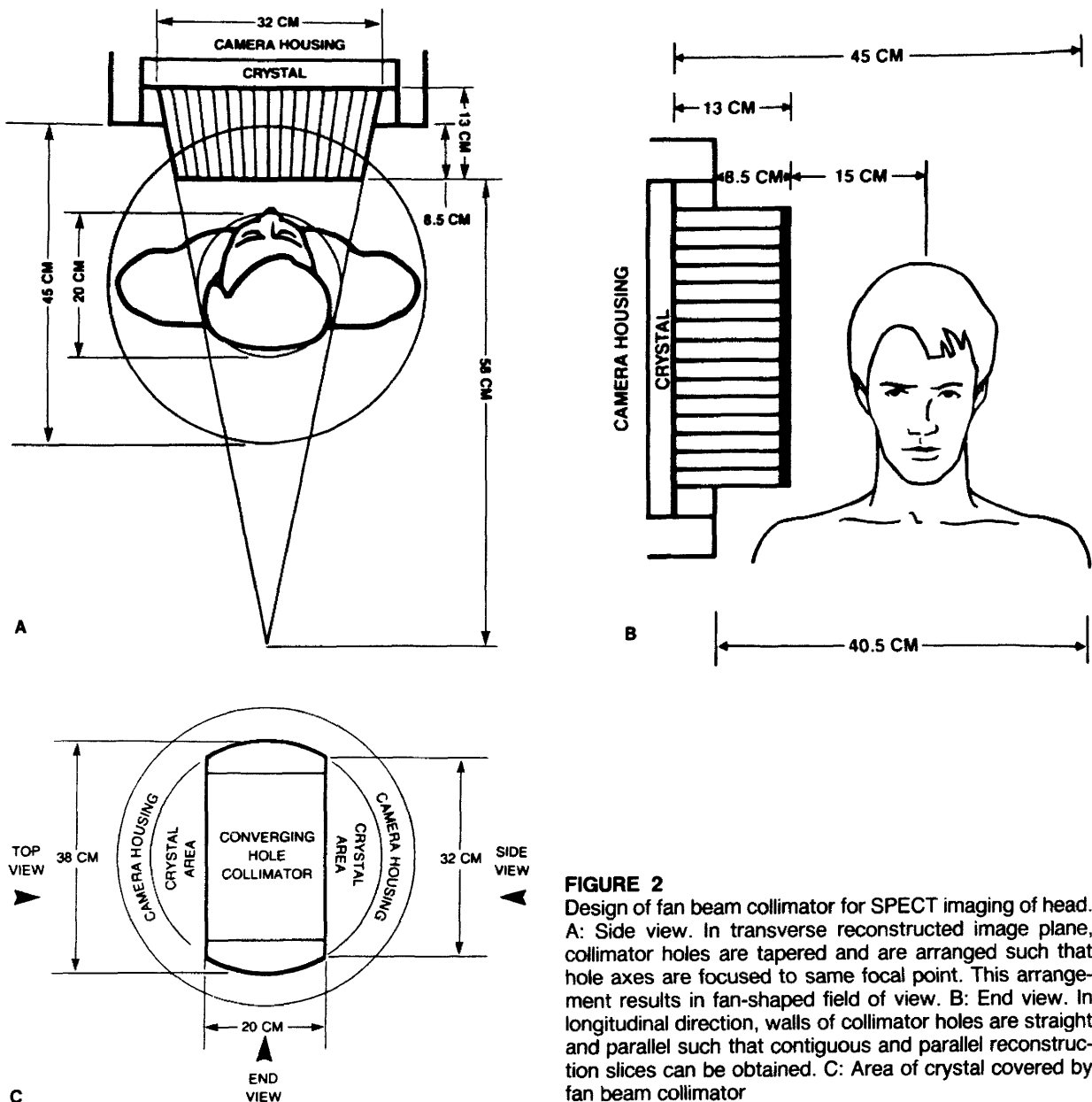


FIGURE 2
 Design of fan beam collimator for SPECT imaging of head. A: Side view. In transverse reconstructed image plane, collimator holes are tapered and are arranged such that hole axes are focused to same focal point. This arrangement results in fan-shaped field of view. B: End view. In longitudinal direction, walls of collimator holes are straight and parallel such that contiguous and parallel reconstruction slices can be obtained. C: Area of crystal covered by fan beam collimator

of the collimator with respect to the crystal area of the scintillation camera is shown in Fig. 2C.

Given the geometric configuration of the fan beam collimator in Fig. 2, simulations using Eqs. (2) to (5) allowed us to determine the hole size for the fan beam collimator for a given spatial resolution and predict the geometric efficiency of the collimator. Specifically, Eqs. (2) and (3) were used to obtain the transfer functions at various source distances for a given hole size. Fourier transformation of the transfer function yielded the line spread functions from which the spatial resolutions in terms of FWHM can be obtained. Once the hole size was specified, the geometric efficiency of the collimator was determined by Eqs. (4) and (5).

Measurements of Physical Characteristics

The physical characteristics of the fan beam collimator were measured for comparison with theoretic predictions. Line spread functions were measured for a 10 cm length of polyethelene tubing (0.38 mm i.d. and 1.14 mm o.d.) filled with technetium-99m (^{99m}Tc) pertechnetate. The line source was oriented perpendicular to the planes of the converging holes and placed on the axis of the fan beam geometry. Images of the line source were collected at different distances from the collimator face both in air and in a water phantom. A 20% window peaked at 140 keV was used. The data were measured with a pixel size at the image plane of 0.16 cm. Images of a pair of line sources with 10 cm spacing were also

collected at the same source distances as in the line spread function measurements. The spacings between the line sources in the images were used to calculate the magnification calibration factor and to determine the sampling intervals at the corresponding distances.

The geometric efficiencies of the fan beam, the LEGP and the HRES collimators were measured using a point source of ^{99m}Tc , placed on the axis of the collimators and at various distances from the collimator face. The results were used for comparison.

Image Reconstruction and Attenuation Correction

The implementation of the image reconstruction algorithm for the fan beam collimator data collection is based on the convolution method (10-15). Projection data at each angle are convolved with the convolution function (15) and are then backprojected. The algorithm corrects for the variations in detection efficiency due to the fan beam geometry. The parameters for the fan beam collimator and for the reconstruction geometry are determined (15). They included the focal length of the collimator, the radius of rotation, the location of the focal point projected onto the projection data, and the center of rotation with respect to the axis of the fan beam geometry.

The attenuation correction algorithm developed for the image reconstruction of the fan beam data is based on the preprocessing correction method (16). An elliptical body contour was determined by a nonlinear data fitting technique (17). Assuming the attenuation coefficient is constant inside the elliptical body contour, the projection data are corrected for attenuation before the reconstruction algorithm is applied.

Phantom Studies

To evaluate the performance of the fan beam collimator and the image reconstruction algorithm, phantom studies were performed. The SPECT phantom[‡] consists of a 20-cm diameter cylindrical container which is filled with water. The top half of the phantom contains six arrays of plastic rods with diameters ranging from 4.8 to 12.7 mm and arranged into six pie-shaped patterns. The lower half contains an array of six plastic spheres with diameters ranging from 9.5 to 31.8 mm. By injecting radionuclides of ^{99m}Tc in the phantom, the rod and sphere patterns appear as cold regions with various sizes in the image.

During data collection, the axis of the SPECT phantom is placed at a distance of 15 cm from the collimator face and parallel to the axis of rotation. The projection data were collected from 128 views of 64x64 matrices over 360°. A uniform flood image with 30 million total counts was obtained using the fan beam collimator to correct for nonuniformity of the projection data. Reconstructed images were obtained using the fan beam reconstruction algorithm and the attenuation correction method described earlier.

Clinical Studies

Further evaluation of the fan beam collimator was made with clinical studies of the temporomandibular joints (TMJ). Patients were given 15 mCi of ^{99m}Tc labelled HDP intravenously and, 3 hr later, projection data were obtained using both the LEGP and the fan beam collimators. To achieve the best spatial resolution, the radius of rotation was minimized. On the average, the minimum radius of rotation was ~22.5 for the LEGP collimator and 15 cm for the fan beam collimator. The projection data were digitized in 64x64 matrices. This gave a reconstructed pixel size of 6.4 mm for the LEGP and 3.8 mm for the fan beam collimators. A total of 128 views over 360° around the patient's head were collected. The acquisition time per view was 10 seconds resulting in a total imaging time of about 25 min per collimator study. Image reconstruction and attenuation correction methods described earlier were applied to obtain the reconstructed images with slice thickness equal to 6.4 mm in both studies.

RESULTS AND DISCUSSION

Prototype Fan Beam Collimator

The construction of the fan beam collimator used corrugated sheets of lead 0.01 in. thick. As shown in Fig. 3, the corrugation forms the converging hole con-

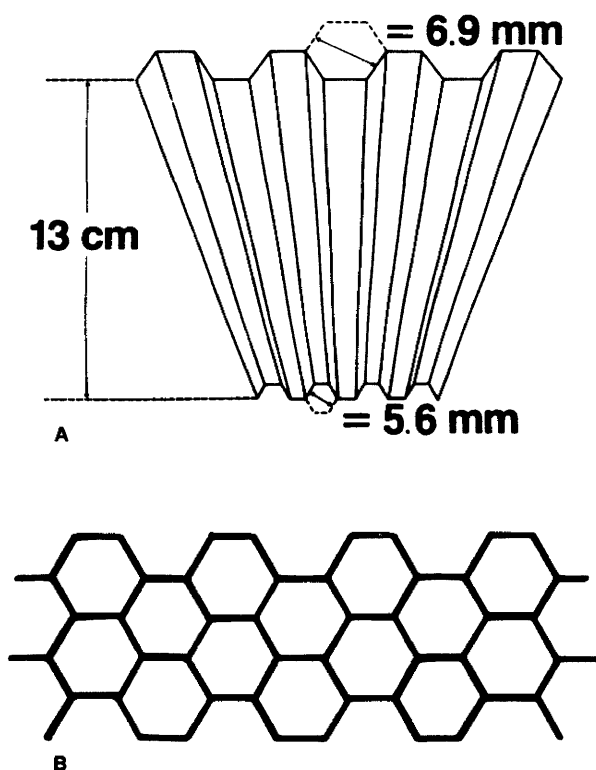


FIGURE 3
Construction of fan beam collimator using corrugated sheets of lead. A: Single corrugated sheet with focused corrugation. B: Fan beam collimator is formed by stacking corrugated sheets

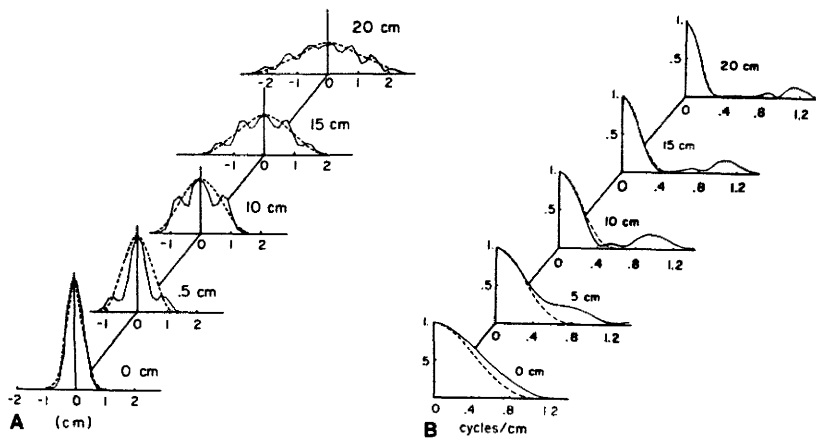


FIGURE 4

A: Measured (—) line spread functions of fan beam collimator are compared with theoretic (---) predictions as function of source distance. B: Transfer functions of fan beam collimator, calculated from measured line spread functions, are compared with theoretic predictions

figuration and produces tapered collimator holes with hexagonal shape when the sheets are stacked and glued together. Also, the uniform thickness of the corrugation forms the parallel sides of the collimator holes in the longitudinal direction with double-thickness walls on opposed sets of flats where the corrugated sheets abut. Based on the design objective and related theory, the hexagonal hole at the central axis of the collimator has a flat-to-flat dimension of 6.9 mm at the base and 5.6 mm at the face of the collimator.

Spatial Resolution and Geometric Efficiency

Figure 4A shows examples of the line spread function measurements in air and Fig. 4B shows the corresponding transfer functions. In using a sampling width of 1.6 mm in the measurements, the effect of the long colli-

imator septa is shown as ripples superimposed on the line spread functions and as an increase in the high frequency component in the transfer function. In the actual SPECT data collection, however, when a sampling size of 6.4 mm is used, the ripples are averaged out. This is demonstrated in the response functions at a source distance of 15 cm shown in Figs. 5A and B. Excellent agreement between measured and theoretic predictions are obtained.

Figure 6A shows the spatial resolution of the fan beam collimator design (in terms of FWHM) as a function of source distance in comparison with the parallel hole LEGP and HRES collimators. The FWHM values of the predicted line spread function for the fan beam collimator were derived from Eqs. (2) and (3) using the design parameters shown in Fig. 2 and the

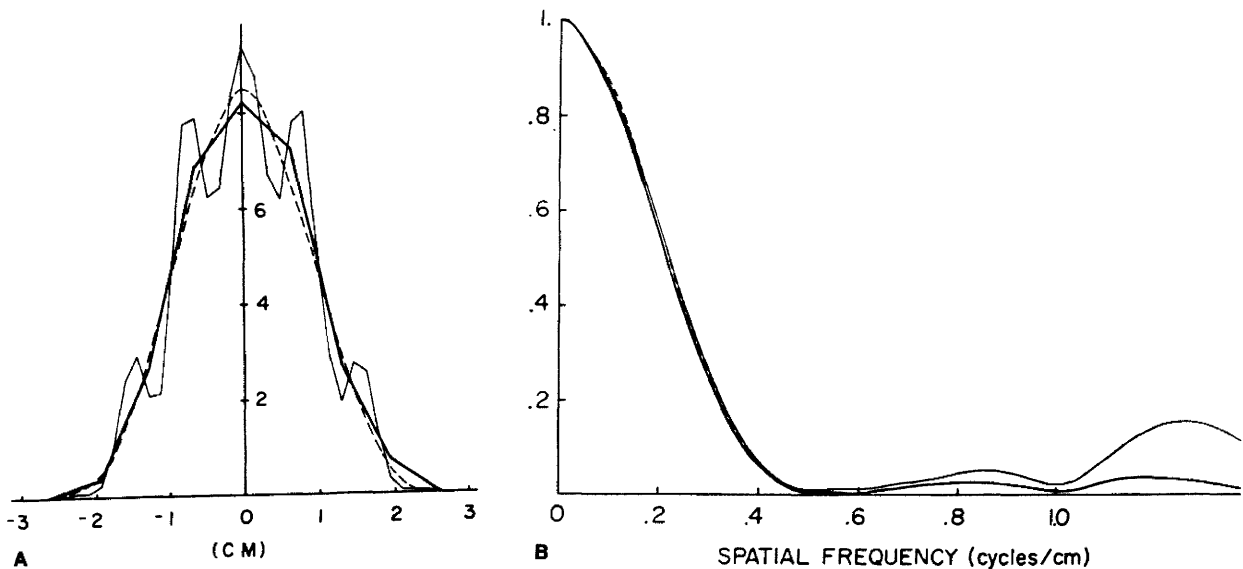


FIGURE 5

A: Effect of sampling size on measured line spread functions of fan beam collimator. At sampling size of 6.4 mm in actual SPECT data collection, ripples shown in Fig. 4A (—) are averaged out (—). B: Effect of sampling size on transfer functions of fan beam collimator. (---) Represents theoretical prediction

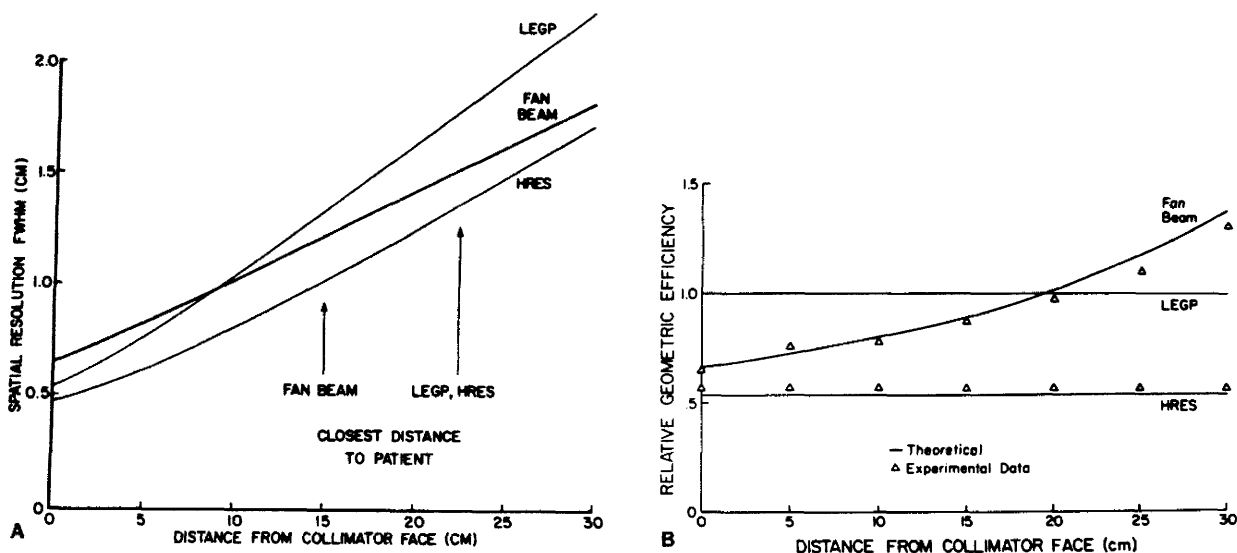


FIGURE 6

A: Spatial resolution (FWHM of line spread function) of fan beam collimator compared with LEGP and HRES collimators. Design of fan beam collimator allows closest distance between collimator and patient. At closest distances spatial resolution of fan beam collimator is equal to that of high resolution collimator. B: Geometric efficiency of fan beam collimator compared with LEGP and HRES collimators. Solid lines are obtained from theoretic predictions, and symbol Δ represents experimental data

method described earlier. When the conventional parallel hole collimators are used, the patient's shoulders restrict the radius of rotation to a minimum of 22.5 cm. At this distance of radius of rotation, the spatial resolution is ~18 mm for the LEGP and 13.5 mm for the HRES collimators, respectively. The extended hole design as shown in Fig. 1 allows the radius of rotation to be as short as 15 cm for the fan beam collimator with a spatial resolution of 12 mm.

In Fig. 6B, the theoretic geometric efficiency of the fan beam collimator [Eqs. (4) and (5)] is shown as a solid line. This was normalized with respect to that of the LEGP collimator. The measured sensitivity of the LEGP collimator is ~330 cpm/ μ Ci. The geometric efficiency of the HRES collimator normalized with respect to that of the LEGP collimator is also plotted for comparison. At 15 cm from the collimator face the geometric efficiency of the fan beam collimator equals ~85% of that of the LEGP and is ~55% higher than that of the HRES collimator.

Image Reconstruction and Attenuation Correction

The reconstruction algorithm and attenuation correction method were initially implemented on the GE STAR computer system⁸ in Fortran code. The processing times per 64×64 image slice with 128 projection angles were ~2 min and ~2½ min for reconstruction with and without attenuation correction, respectively. To increase computational speed, the reconstruction software was implemented on an array processor⁹ in assembly code. By taking advantage of the parallel and pipeline processing capabilities of the array processor, we were able to cut the processing time per 64×64

slice for reconstruction without attenuation correction to ~6 sec. Presently, the attenuation correction method is still coded in FORTRAN and requires ~30 sec of additional processing time.

Phantom Studies

Figure 7A shows the reconstructed images of the SPECT phantom without applying a preprocessing filter to the projection data. Images in the right and left columns have been processed with and without attenuation correction, respectively. Figure 7B shows the same results but with a 3×3 smoothing filter applied to the projection data. The total counts are about 18 million in the images through the rod pattern by averaging over four slices and about 9 million in the images of the spheres by averaging over two slices. The phantom images in Fig. 7 demonstrate the good image quality obtainable with the fan beam collimator and the image reconstruction algorithm.

Patient Studies

Figures 8A and B show the reconstructed transaxial images of the temporomandibular joint (TMJ) from the same patient using the LEGP and fan beam collimators. The levels of the SPECT slices are carefully matched for optimal comparison. In general, better detail of the anatomy of the bone structure is visible in the reconstructed images obtained with the fan beam collimator. Although increased uptake is seen in the right TMJ with LEGP images, the details of the abnormal uptake are better demonstrated by the fan beam images. Such improved resolution is clinically relevant since we are able to determine that, in this case, the lateral aspect of the TMJ is involved.

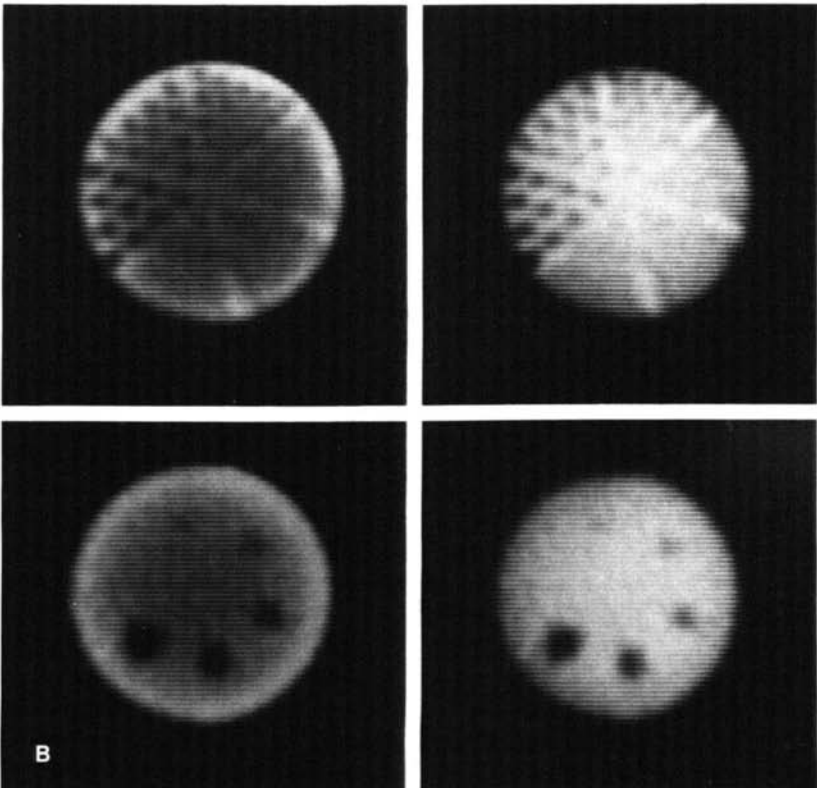
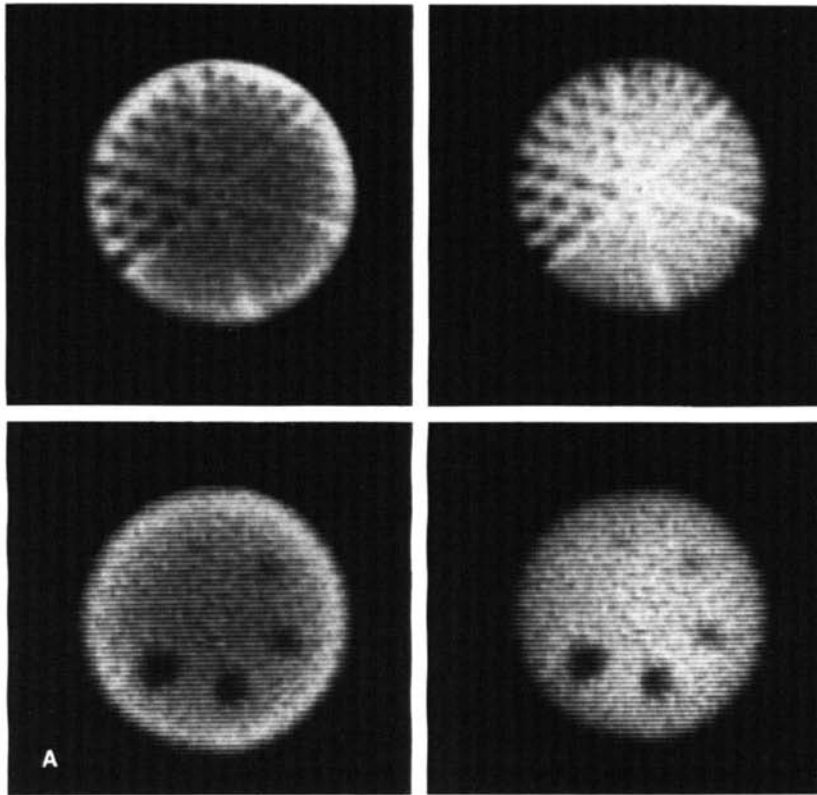


FIGURE 7
 Reconstructed images of SPECT phantom obtained from using fan beam collimator. Images in the right and left columns were processed with and without attenuation correction, respectively. In images of rod pattern and of spheres, total counts are ~18 million and 9 million, respectively. A: No filtering. B: Projection data had been smoothed with a 3x3 smoothing filter

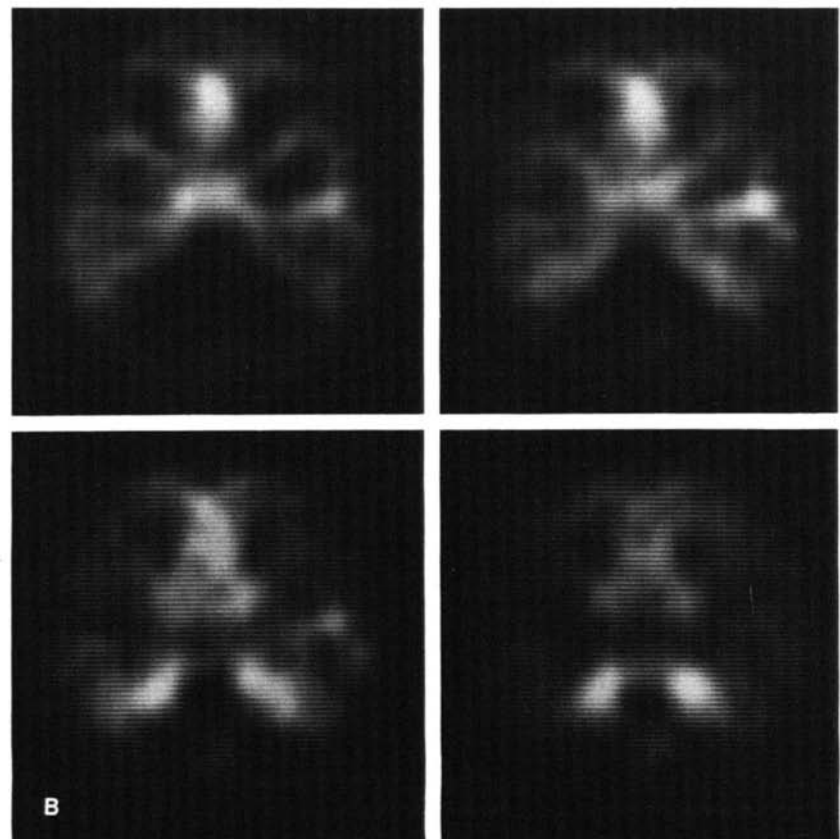
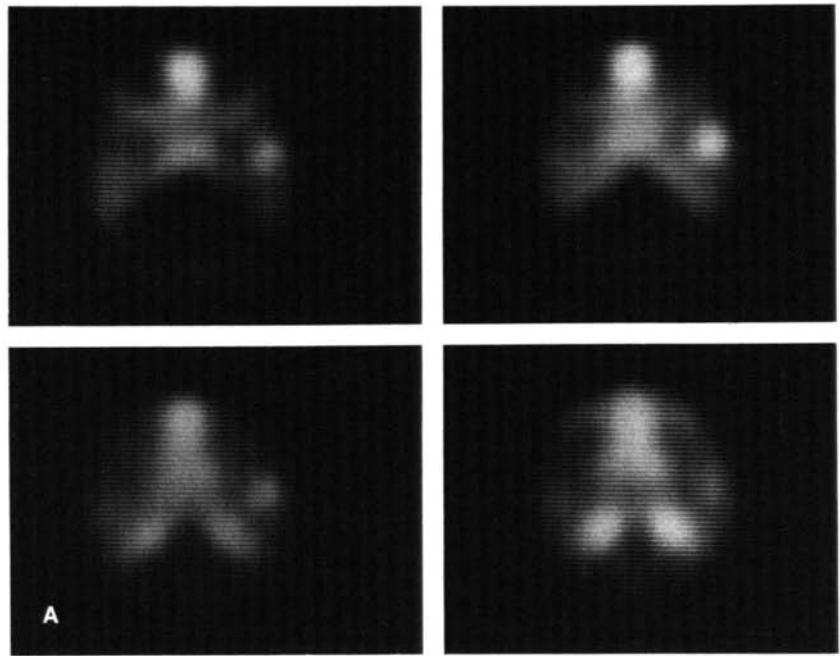


FIGURE 8
 Reconstructed images from patient with right TMJ disease, using LEGP (8A) and fan beam (8B) collimators. While increased uptake in right TMJ is evident in both sets of images, fan beam images demonstrate involvement of lateral portion of joint

SUMMARY

We have demonstrated the clinical utility of a long bore fan beam collimator which was designed and constructed for SPECT imaging of the head using a commercial system. At normal operating radii of rotation, the fan beam collimator provides about the same spatial resolution as the HRES collimator and with geometric efficiency equal to ~85% of that of the LEGP collimator. A fan beam reconstruction algorithm and attenuation correction method were implemented. Processing time was decreased significantly by implementing the reconstruction algorithm in an array processor. Images produced through phantom studies are of good quality and void of artifacts. Initial clinical studies on the TMJ demonstrate superior reconstructed image quality obtained with the fan beam as compared with the LEGP collimator.

Due to the thick camera housing of the commercial SPECT system, the collimator utilizes long holes to avoid the patient's shoulder during camera rotation and at the same time to draw close to the patient's head. However, the extended hole design results in lower geometric efficiency as compared to a design with the same spatial resolution but shorter hole length. For a camera with thinner housing that will clear the patient's shoulders (1), a fan beam collimator can be designed with the same hole length and spatial resolution of the LEGP collimator but having a 1.6 gain in geometric efficiency. The method of collimator design described in this paper can be applied to this design and other fan beam collimators in general.

FOOTNOTES

[†] General Electric Co., (General Electric 400 A/T), Medical Systems Group, Milwaukee, WI.

[‡] Data Spectrum Corp. SPECT phantom, Deluxe Model (Model No. 5000), Chapel Hill, NC.

[§] General Electric Co. Medical Systems Group, Milwaukee, WI. The GE STAR computer system consists of a Data General NOVA 4× 16 bit minicomputer with 32 K core memory.

[¶] General Electric Co. Medical Systems Group, (Analogic AP400 24 bit block floating array processor), Milwaukee, WI.

REFERENCES

1. Larsson SA, Bergstrand G, Bergstedt H, et al: A special cut-off gamma camera for high-resolution SPECT of the head. *J Nucl Med* 25:1023-1030, 1984
2. Polak JF, Holman BL, Moretti J-L, et al: I-123 HIPDM brain imaging with a rotating gamma camera

- and slant-hole collimator. *J Nucl Med* 25:495-498, 1984
3. Jaszczak RJ, Chang L-T, Murphy PH: Single photon emission computed tomography using multi-slice fan beam collimator. *IEEE Trans Nucl Sci NS-26(1):610-618*, 1979
4. Lim CB, Chang LT, Jaszczak RJ: Performance analysis of three camera configurations for single photon emission computed tomography. *IEEE Trans Nucl Sci NS-27(1):559-568*, 1980
5. Anger HO: Scintillation camera with multichannel collimators. *J Nucl Med* 5:515-531, 1964
6. Metz CE, Atkins FB, Beck RN: The geometric transfer function component for scintillation camera collimators with straight parallel holes. *Phys Med Biol* 25:1059-1070, 1980
7. Muehllehner G, Dudeh J, Moyer R: Influence of hole shape on collimator performance. *Phys Med Biol* 21:242-250, 1976
8. Tsui BMW, Gunter DL, Beck RN: Study of spatial resolutions in single-photon ECT. *J Nucl Med* 23:P45, 1982 (abstr)
9. Kiros CT, Leonard PF, Keyes JW: An optimized collimator for single photon computed tomography with a scintillation camera. *J Nucl Med* 19:322-323, 1978
10. Herman GT, Lakshminarayanan AV, Naparstek A: Convolution reconstruction techniques for divergent beams. *Comp Biol Med* 6:259-271, 1976
11. Herman GT, Lakshminarayanan AV, Naparstek A: Reconstruction using divergent-ray shadowgraphs. In *Reconstruction Tomography in Diagnostic Radiology and Nuclear Medicine*, Ter-Pogossian MM, et al., eds. Baltimore, University Park Press, 1977, pp 105-117
12. Huesman RH, Gullberg GT, Greenberg WL, et al: RECLBL Library Users Manual—Donner Algorithms for Reconstruction Tomography, Lawrence Berkeley Laboratory Publication PUB 214, 1977
13. Pang SC, Genna S: A Fourier convolution fan-geometry reconstruction algorithm: Simulation studies, noise propagation, and polychromatic degradation. In *Reconstruction Tomography in Diagnostic Radiology and Nuclear Medicine*. Ter-Pogossian MM, et al., eds. Baltimore, University Park Press, 1977, pp 119-137
14. Herman GT, Naparstek A: Fast image reconstruction based on a Radon inversion formula appropriate for rapidly collected data. *SIAM. J Appl Math* 33:511-533, 1977
15. Gullberg GT, Crawford CR, Tsui BMW: Reconstruction algorithm for fan beam with a displaced center-of-rotation. *IEEE Trans Med Imaging MI-5(1):23-29*, 1986
16. Budinger TF, Gullberg GT, Huesman RH: Emission computed tomography. In *Image Reconstruction From Projections: Implementation and Applications*, Herman GT, Ed. New York, Springer Verlag, 1979, pp 147-246
17. Gullberg GT, Malko JA, Eisner RL: Boundary determination methods for attenuation correction in single photon emission computed tomography. In *Emission Computed Tomography: Current Trends*, Esser PD, Westerman BR, eds. New York, The Society of Nuclear Medicine, 1983, pp 33-53